Inorganic Chemistry

ARTICLE

pubs.acs.org/IC

Iron(II) Cage Complexes of N-Heterocyclic Amide and Bis(trimethylsilyl)amide Ligands: Synthesis, Structure, and Magnetic Properties

Scott A. Sulway, David Collison, Joseph J. W. McDouall, Floriana Tuna, and Richard A. Layfield*

School of Chemistry, The University of Manchester, Oxford Road, Manchester M13 9PL, U.K.

Supporting Information

ABSTRACT: Metallation of hexahydropyrimidopyrimidine (hppH) by $[Fe\{N(SiMe_3)_2\}_2]$ (**1**) produces the trimetallic iron(II) amide cage complex $[\{(Me_3Si)_2NFe\}_2(hpp)_4Fe]$ (**2**), which contains three iron(II) centers, each of which resides in a distorted tetrahedral environment. An alternative, one-pot route that avoids use of the highly air-sensitive complex **1** is described for the synthesis of the iron(II)−lithium complex $[\{(Me_3Si)_2N\}_2Fe\{Li(bta)\}]_2$ (**3**) (where btaH = benzotriazole), in which both iron(II) centers reside in 3-coordinated pyramidal environments. The structure of **3** is also interpreted in terms of the ring laddering principle developed for alkali metal amides. Magnetic susceptibility measurements reveal that both compounds display very weak antiferromagnetic exchange between the iron(II) centers, and that the iron(II) centers in **2** and **3** possess large negative axial zero-field splittings.

INTRODUCTION

The iron(II) amide $[Fe\{N(SiMe_3)_2\}_2]$ (**1**)[1] is a landmark compound that has stimulated extensive investigations into low-coordinate iron chemistry.[2,3] In addition to the fundamental interest in the coordination chemistry of iron complexes with bulky amide ligands, the reactions of **1** with a broad range of E−H acidic substrates have enabled systematic studies of low-coordinate iron complexes containing nitrogen,[4−10] oxygen,[11,12] phosphorus,[13] sulfur,[9,10,14−22] or selenium[23,24] donor ligands. Chaudret et al. have recently shown that **1** can also be thermally decomposed in an atmosphere of dihydrogen in the presence of long-chain acids and long-chain amines to produce monodisperse iron nanoparticles.[25,26]

The reactions of **1** with thiols and elemental sulfur have attracted particular interest, because of the range of structurally diverse iron−sulfur cage compounds that can be accessed via this synthetic route.[17,20,22] However, synthetic routes to polymetallic iron cage compounds in which the iron centers are bridged by amido nitrogens have hitherto not been reported. Previous studies on the synthesis of manganese(II) amide cages from the deprotonation of functionalized aromatic primary amines by manganocene[27] suggested that iron(II) amide cage compounds should be accessible using **1** as the precursor. Thus, our interest in **1** stems from the Brønsted basic reactivity of the $[(Me_3Si)_2N]^-$ ligands toward heterocycles that contain acidic N−H groups, and the potential for this reactivity to be applied in the synthesis of iron(II) cages. Furthermore, we recently reported that deprotonation of the N-heterocycle benzotriazole (btaH) by *tris*(cyclopentadienyl)dysprosium forms the dimeric complex $[Cp_2Dy(\mu\text{-bta})]_2$, a complex which shows single-molecule magnet (SMM) behavior,[28,29] hence given the current interest in SMMs based on 3d transition metals, it is conceivable that the chemistry of **1** could be developed to provide an alternative synthetic method in the SMM field.

We now report the trimetallic iron(II) amide cage complex $[\{(Me_3Si)_2NFe\}_2(hpp)_4Fe]$ (**2**) and the tetrametallic iron(II)−lithium complex $[\{(Me_3Si)_2N\}_2Fe\{Li(bta)\}]_2$ (**3**) (where $[hpp]^-$ = hexahydropyrimidopyrimidide, $[bta]^-$ = benzotriazolide). Compounds **2** and **3** were characterized by X-ray crystallography, SQUID magnetometry, and NMR spectroscopy, and DFT (density functional theory) calculations were carried out on compound **2**.

RESULTS AND DISCUSSION

Synthesis and Structural Characterization. The reaction of **1** with (hpp)H produced a brown solution, which, after being concentrated and stored at −30 °C, yielded yellow−green crystalline needles. X-ray crystallography revealed the product to be the trimetallic iron(II) cage complex **2** (see Scheme 1 and Figure 1).

In the structure of **2**, the central Fe(2) atom resides in a distorted tetrahedral environment through complexation by four N-donor atoms of the $[hpp]^-$ ligands. Of the four N-donor

Scheme 1. Synthesis of Compound 2

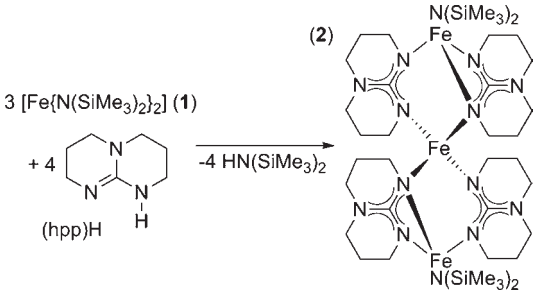

Received: November 23, 2010
Published: February 11, 2011

   dx.doi.org/10.1021/ic102341a | *Inorg. Chem.* 2011, 50, 2521–2526

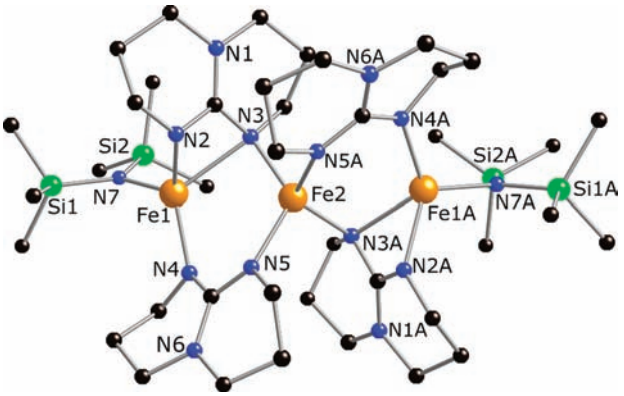

Figure 1. Molecular structure of compound **2**. Hydrogen atoms are omitted for the sake of clarity.

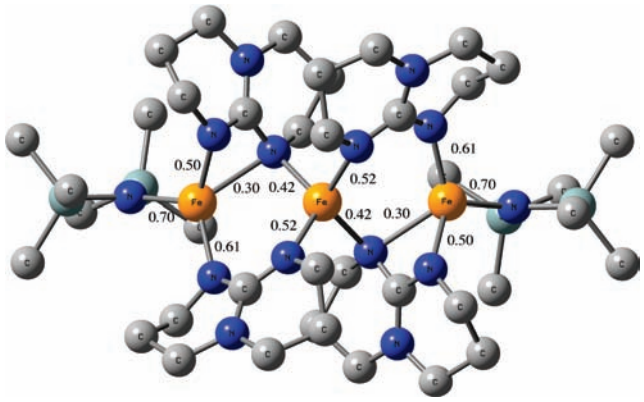

Figure 2. Mayer bond order (B3LYP/Def2-SVP) analysis for compound **2**.

atoms coordinated to Fe(2), N(5) and N(5A) engage in end-on bonding, with the Fe(2)−N(5/5A) distance being 2.0409(19) Å, whereas N(3) and N(3A) also μ-bridge to Fe(1) and Fe(1A) to result in Fe(2)−N(3/3A) and Fe(1)−N(3/3A) distances of 2.1064(18) and 2.3066(18) Å, respectively. The coordination geometry of Fe(1) is also a distorted tetrahedron, consisting of a κ^2-[hpp]$^-$ ligand that coordinates through N(2) and N(3), a κ^1-[hpp]$^-$ ligand that coordinates through N(4), and a terminal [$(Me_3Si)_2N$]$^-$ ligand that coordinates to Fe(1) through N(7). The resulting Fe−N distances are as follows: Fe(1)−N(2), 2.0645(19) Å; Fe(1)−N(4), 1.9901(19) Å; and Fe(1)−N(7), 1.9880(19) Å. The distorted nature of the tetrahedral iron coordination environments in **2** is apparent from the range of N−Fe−N bond angles. For Fe(1), the N−Fe−N bond angles are 61.95(7)° and 113.98(7)−122.69(8) Å; for Fe(2), the angles are in the range of 101.58(7)°−121.72(7)°. The Fe(1)···Fe(2) separation is 3.127 Å and the Fe(1)−Fe(2)−Fe(1A) angle is 153.86(1)°, which indicates a "bending" of the molecule and leads to C_2 point symmetry. The ^{1}H NMR spectrum of **2** shows a sharp singlet at 2.39 ppm corresponding to the $SiMe_3$ substituents, and resonances at 7.24 and 7.20 ppm due to the hydrogens of the [hpp]$^-$ ligands, suggesting that the solid-state structure is preserved in benzene solution.

Although the coordination chemistry of guanidinate ligands is well established,[30] surprisingly few iron complexes of these ligands are known,[31] and complex **2** is the first iron complex of the anionic [hpp]$^-$ ligand. Two iron complexes of neutral hpp-

Scheme 2. Synthesis of Compound 3

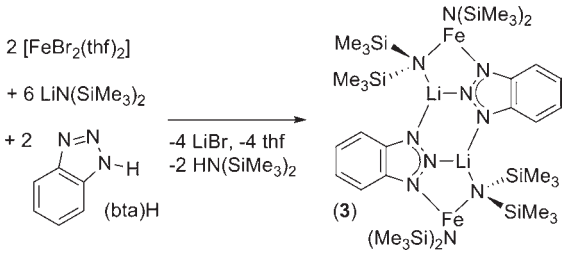

type ligands related to **2** are [{hpp(H)}$_2$FeCl$_2$] and [{H_2C(hpp)}$_2$FeCl$_2$], each of which contains an iron(II) center in a tetrahedral environment, with the hpp ligands coordinated through imino nitrogens.[32] The [hpp]$^-$ ligand is well-known in transition-metal chemistry for its ability to encourage the formation of metal−metal bonds, with compounds having the general formula of [M_2(hpp)$_4$] being particularly prevalent.[33] A search of the Cambridge Structural Database reveals that more than half of the transition-metal complexes of the [hpp]$^-$ contain a metal−metal bond.[34]

However, the Fe···Fe separation of 3.127 Å in **2** is too large for an Fe−Fe bond to be feasible. Indeed, a Mayer bond order analysis confirms that the iron centers in **2** only bond to nitrogen (see Figure 2), while the Fe···Fe interactions show bond orders of only 0.06.

A drawback with **1** is its extremely high sensitivity to air. We have found that an alternative, "one-pot" approach has potential to be developed as a general synthetic route to iron(II) cages. With this method, we combined the N−H acidic heterocycle benzotriazole (bta)H, which is known to encourage cage formation,[35] with solid [$FeBr_2$(thf)$_2$] and the somewhat less air-sensitive lithium bis(trimethylsilyl)amide (although care was still taken to exclude oxygen and moisture from the reaction). The solids were cooled to −78 °C and then a toluene was added. The reaction developed a green color upon warming to room temperature, which then became brown and was accompanied by the formation of a precipitate. Filtering the reaction and storing the concentrated solution at −30 °C produced green crystals, which X-ray crystallography revealed to be [{$(Me_3Si)_2N$}$_2$-Fe{Li(bta)}]$_2$ (**3**) (see Scheme 2 and Figure 3).

The molecular structure of **3** is a centrosymmetric dimer that consists of a central {Li(bta)}$_2$ core capped on each end by one [Fe{$N(SiMe_3)_2$}$_2$] unit. Combining the two {Li(bta)} units in the center of **3** generates a 6-membered Li_2N_4 ring with the Li(1)−N(2) and Li(1)−N(3A) distances being 2.044(5) and 1.992(5) Å, respectively. A μ-{$N(SiMe_3)_2$} ligand links the {Li(bta)} core to the iron amide capping unit to result in an Li(1)−N(4) bond distance of 2.109(5) Å, and an Li(1)−N(4)−Fe(1) angle of 93.73(15)°. The Fe(1) atom in **3** resides in a distorted pyramidal environment, with the Fe(1)−N(1), Fe(1)−N(4), and Fe(1)−N(5) distances being 2.052(2), 1.9764(19), and 1.909(2) Å, respectively, and the N(1)−Fe−N(4), N(4)−Fe−N(5) and N(5)−Fe−N(1) angles being 104.50(8)°, 141.31(9)°, and 112.55(9)°. The Fe(1/1A) centers are positioned 0.13 Å out of the plane of their three respective nitrogen donor atoms. A sharp singlet at 0.11 ppm in the ^{1}H NMR spectrum of **3** can be assigned to the $SiMe_3$ substituents, but the resonances due to the [bta]$^-$ protons are less distinct, with a weak, broad signal being observed at −11.2 ppm ($\omega_{1/2}$ = 380 Hz).

dx.doi.org/10.1021/ic102341a |*Inorg. Chem.* 2011, 50, 2521–2526

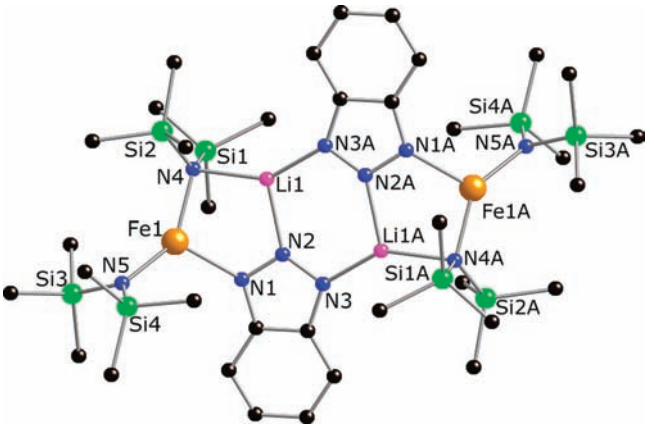

Figure 3. Molecular structure of compound **3**. Hydrogen atoms are omitted for the sake of clarity.

Alkali metal amido ferrate complexes have recently been shown to display interesting applications in synthesis,[36] although crystallographically authenticated structures such as that of **3** are scarce.[36b] The $\{Li(bta)\}_2$ core of **3** is isostructural with the $\{Li(bta)\}_2$ units found in the polymeric ladder structure of $[(dmso)Li(bta)]_\infty$ (**4**) (where dmso = dimethylsulfoxide) (see Scheme 3).[37] While crystalline **4** could only be obtained by dissolving $[Li(bta)\cdot thf]$ in hot dmso, the $SiMe_3$ substituents in **3** result in good solubility in toluene at room temperature. Because the polymeric structure of $[(dmso)Li(bta)]_\infty$ can be interpreted in terms of the ring laddering principle developed for alkali-metal amides,[38] the central $\{Li(bta)\}_2$ core in **3** can be regarded as an intercepted dimeric unit of the $[Li(bta)]_\infty$ ladder. However, whereas structural studies on intercepted alkali-metal amide ladders normally deploy tertiary amines as the interceptors, in **3**, the intercepting units are molecules of $[Fe\{N(SiMe_3)_2\}_2]$. This interpretation gives insight into the mechanism through which **3** is formed. The first component to form is probably $[Fe\{N(SiMe_3)_2\}_2]$, through transmetallation of $[FeBr_2(thf)_2]$ by $LiN(SiMe_3)_2$, which also explains the initial green color of the reaction mixture. The second step is the deprotonation of btaH by the remaining $LiN(SiMe_3)_2$ to generate $[Li(bta)]$, which then dimerizes but cannot polymerize, because of the presence of the $[Fe\{N(SiMe_3)_2\}_2]$ traps, leading to a third step in which molecules of **3** form (see Scheme 3). The formation of **3** could be of general significance, because it may be possible to trap units of other alkali-metal amide ladders with other low-coordinate metal silyl-amides.

Magnetochemistry and DFT Calculations. Magnetic susceptibility measurements were carried out on polycrystalline samples of compounds **2** and **3** in an applied field of 0.1 T (see Figure 4). For compound **2**, the room-temperature $\chi_M T$ value of 9.6 cm^3 K mol^{-1} corresponds to three uncoupled tetrahedral Fe(II) d^6 centers in **2**. Upon cooling, $\chi_M T$ decreases smoothly to 8.94 cm^3 K mol^{-1} at 50 K and then more rapidly to reach 3.87 cm^3 K mol^{-1} at 2 K. In addition, the temperature dependence of the susceptibility of **2** shows a continuous increase between 300 K (χ_M = 0.031 cm^3 mol^{-1}) and 2 K (χ_M = 0.193 cm^3 mol^{-1}), without showing a maximum above 1.8 K, suggesting a very weak antiferromagnetic exchange between Fe(1/1A) and Fe(2). Fitting the susceptibility data with the Curie−Weiss law, $\chi_M = C/(T-\theta)$, gave values of C = 9.6 cm^3 K mol^{-1} and θ = −3.4 K (or −2.4 cm^{-1}), where C and θ represent the Curie constant and the Weiss temperature, respectively. The value of C is in agreement with the presence of three tetrahedral Fe(II) ions with S = 2, and the negative θ value indicates some antiferromagnetic exchange in **2**.

Scheme 3

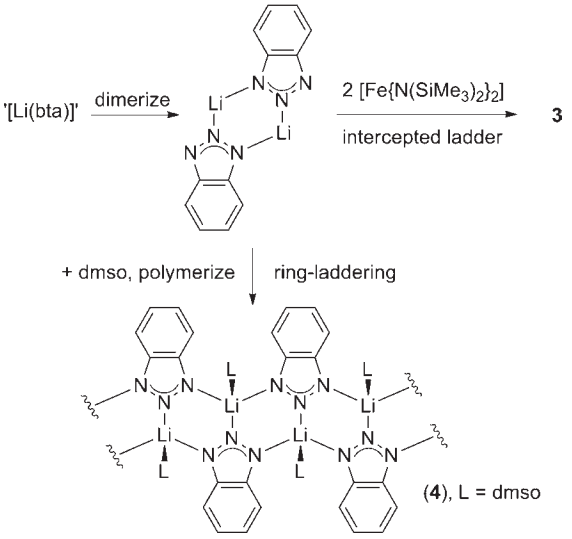

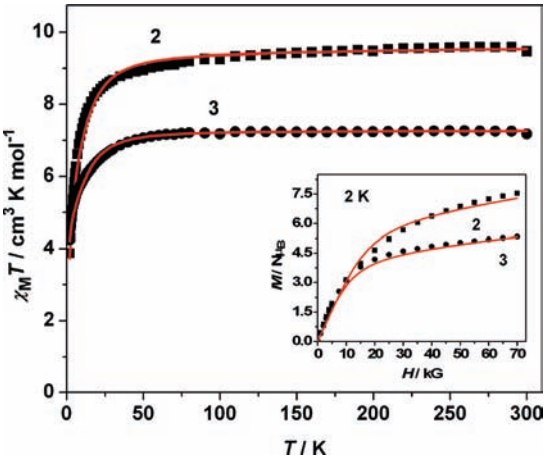

Figure 4. Plots of $\chi_M T$ vs temperature and of magnetization versus field at 2 K (inset) for **2** and **3**.

The magnetization of **2** increases with increasing field at 2 K to reach 7.28 $N\mu_B$ at 70 kG, but does not saturate (see Figure 4, inset), and the data could only be modeled by taking into account axial (D) and rhombic (E) zero-field splitting (ZFS) terms, according to the following equation (eq 1):[39]

$$H = -2J\sum_{i<j} S_i S_j + D\sum\left[S_{iz}^2 - \frac{1}{3}S_i(S_i+1)\right] + E\sum\left[S_{ix}^2 - S_{iy}^2\right] \quad (1)$$

Applying this equation to the susceptibility and magnetization data for **2** produced values of J = −0.08 cm^{-1}, D = −10.2 cm^{-1}, $|E|$ = 0.06 cm^{-1}, and g = 2.05. The red traces in Figure 4 represent the data as modeled with MAGPACK,[39] using these parameters.

dx.doi.org/10.1021/ic102341a |Inorg. Chem. 2011, 50, 2521–2526

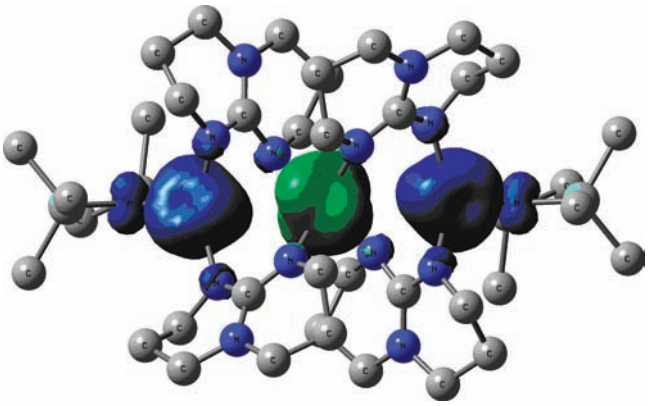

Figure 5. B3LYP/Def2-SVP spin density plot for compound **2** (isosurface value = 0.004 a.u.).

The large value of D implies considerable orbital angular momentum within the d^6 configurations of the Fe(II) centers in **2**, and the nonzero value of E likely reflects the distorted tetrahedral iron coordination geometries. The negative sign of J, the exchange coupling constant, is consistent with antiferromagnetic coupling between Fe(1/1A) and Fe(2). However, this exchange interaction is small, as indicated by the small value of J.

A DFT study of **2** determined that Fe(1/1A) and Fe(2) carry Mulliken spin densities of +3.72 and −3.76, respectively, with the remaining spin density being distributed over the other atoms. Thus, each Fe(II) center in **2** carries four spins ($S = 2$), and the spin density plot (Figure 5) reveals the Fe(1/1A) to be spin up and Fe(2) to be spin down.

Of the various spin states available to **2**, DFT clearly predicts the antiferromagnetically coupled $S = 2$ state to be the most stable, in agreement with the experimental susceptibility data. The plots of $\chi_M T$ versus temperature and of magnetization versus field for **3** shows a decrease in $\chi_M T$ from 7.2 cm^3 K mol^{-1} at 300 K to 4.2 cm^3 K mol^{-1} at 2 K, and the isothermal M versus H plot at 2 K reaches 5.3 Nμ_B at 70 kG and shows no saturation. Simulation of the susceptibility and magnetization data using the spin Hamiltonian described in eq 1 gives $J = -0.03$ cm^{-1}, $D = -10.5$ cm^{-1}, $E = 0$, and $g = 2.2$, with the large value of the axial ZFS once again indicating the presence of orbital angular momentum.

It is noteworthy that compounds **2** and **3** possess very similar, large ZFS values, despite the differing iron(II) coordination geometries in each complex. Additional insight into this observation was not possible with Q-band EPR spectroscopy, because the spectra of each compound consist only of weak resonances, although the absence of a resonance at $g = 2$ is consistent with a large ZFS. However, it has been shown that the large orbital contribution to the angular momentum in three coordinate, distorted trigonal-planar, high-spin iron(II) complexes arises from the effect of spin−orbit coupling in the magnetic field between the low-lying, but nondegenerate d_{z^2} (doubly occupied) and d_{yz} (singly occupied) orbitals,[40] which we propose to explain the large magnitude of the ZFS in **3**. Analysis of the d-orbital structure in **2** does in fact produce a similar picture to that found in 3-coordinated iron complexes (see Table S1 in the Supporting Information), with one essentially doubly occupied d orbital with z^2 character and four singly occupied d orbitals with large d_{yz} character per iron(II) center, which can ultimately be used to rationalize the similar ZFS values in **2** and **3**.

CONCLUSION

In summary, $[Fe\{N(SiMe_3)_2\}_2]$ (**1**) has been used as a precursor to the trimetallic iron(II) amide cage compound $[\{(Me_3Si)_2NFe\}_2(hpp)_4Fe]$ (**2**). An alternative, one-pot synthetic route has been used to synthesize the iron(II)−lithium complex $[\{(Me_3Si)_2N\}_2Fe\{Li(bta)\}]_2$ (**3**). Despite the differing iron coordination geometries in **2** and **3**, their ZFS values were found to be similar, which is an observation that was rationalized in terms of their respective Fe(II) centers possessing similar d-orbital structures. Complexes **2** and **3** contain one and two potentially reactive $[N(SiMe_3)_2]^-$ ligands, respectively, which suggests that they themselves could be developed as precursors to iron(II) amide cages of even higher nuclearity. Our ongoing research will develop this chemistry.

EXPERIMENTAL SECTION

Synthetic Methods, Physical Measurements, and Calculations: General Considerations. All reactions were performed with rigorous exclusion of oxygen and moisture, using standard Schlenk techniques. $[Fe\{N(SiMe_3)_2\}_2]$ (**1**) was prepared according to a literature procedure.[1] Solvents were dried and degassed using an Innovative Technologies Solvent Purification System. ^{1}H NMR spectra were recorded on a Bruker Avance III 400 MHz spectrometer, and UV/vis spectra were recorded on a Shimadzu UV-2401 instrument. Elemental analysis results were obtained using the elemental analysis service of London Metropolitan University.

*$[\{(Me_3Si)_2NFe\}_2(hpp)_4Fe]$ (**2**).* A solution of $[Fe\{N(SiMe_3)_2\}_2]$ (**1**) (0.77 g, 2.0 mmol) in toluene (10 mL) was added to a solution of hexahydropyrimidopyrimidine (0.28 g, 2.0 mmol) in toluene (15 mL) at −78 °C. The reaction mixture was stirred for 30 min before being slowly warmed to room temperature. After stirring for 4 h, the resulting deep brown solution was filtered (Celite, porosity 3) and the solvent reduced in volume to ∼10 mL. Storage of the solution at −30 °C overnight resulted in the formation of air-sensitive yellow−green crystals of **2** (0.57 g, 28%). Analysis: calcd: C 46.15, H 8.14, N 18.85%; found: C 46.16, H 8.00, N 18.64%. ^{1}H NMR (C_6D_6, 400.23 MHz, δ/ppm): 7.24 and 7.20 ppm, 48 H, hpp; 2.39 ppm, 36 H, $SiMe_3$. UV/vis (toluene), λ_{max} (nm) (ε (dm^3 M^{-1} cm^{-1})): 438 (3450), 298 (9800).

*$[\{(Me_3Si)_2N\}_2Fe\{Li(bta)\}]_2$ (**3**).* As solids, $[FeBr_2(thf)_2]$ (0.72 g, 2.0 mmol), $LiN(SiMe_3)_2$ (0.65 g, 4.0 mmol) and 1*H*-benzotriazole (0.24 g, 2.0 mmol) were combined and cooled to −78 °C, and toluene (30 mL) was then added. The reaction was stirred for 30 min at −78 °C before being warmed slowly to room temperature. The initial green−brown color of the reaction mixture changed to a deep brown color after 2 h of stirring. After 14 h at room temperature, the solution was filtered (porosity 3, Celite) and the solvent volume was reduced in vacuo to ∼12 mL. Storing the resulting brown solution at −30 °C overnight resulted in the formation of air-sensitive green crystals of **3** (1.42 g, 72%). Analysis: calcd: C 43.11, H 8.04, N 13.97%; found: C 43.25, H 8.20, N 13.62%. ^{1}H NMR (C_6D_6, 400.23 MHz, δ/ppm): 0.11 ppm, 36 H, $SiMe_3$; −11.2 ppm, broad, bta. UV/vis (toluene), λ_{max} (ε (dm^3 M^{-1} cm^{-1})): 286 nm (2650).

X-ray Crystallography. X-ray crystallographic data on **2** were collected using synchrotron radiation at the Diamond Light Source (Beamline I19), and data on **3** were collected using an Oxford Instruments XCalibur 2 diffractometer (Table 2). The CCDC references codes are 798917 (**2**) and 798918 (**3**).

Magnetic Susceptibility Measurements. Magnetic susceptibility measurements on polycrystalline samples of both compounds were carried out on a Quantum Design MPMS XL SQUID magnetometer in O-ring-sealed KelF capsules. Data were corrected for

Table 2. Crystal Data for Complexes 2 and 3

	2	3
formula	$C_{47}H_{92}Fe_3N_{14}Si_4$	$C_{18}H_{40}FeLiN_5Si_4$
formula weight	1133.23	501.68
T, K	100(1)	100(2)
wavelength, Å	1.54178	0.71073
crystal system	orthorhombic	monoclinic
space group	*Pccn*	$P2_1/n$
a, Å	22.522(4)	18.0458(7)
b, Å	14.455(3)	8.5059(3)
c, Å	17.979(3)	18.7423(7)
α, deg	90	90
β, deg	90	101.276(4)
γ, deg	90	90
V/Å^3	5853.2(19)	2821.34(19)
Z	4	4
density (calculated), g/cm^3	1.286	1.181
absorption coefficient, μ/mm^{-1}	5.230	0.718
crystal size, mm^3	0.1 × 0.1 × 0.1	0.1 × 0.1 × 0.1
θ range, deg	4.39 to 89.23	2.79−28.45
reflections collected	26727	10747
independent reflections	6621	7065
R(int)	0.0309	0.0688
% completeness	98.8	98.1
data/restraints/parameters	6621/0/316	7065/0/274
goodness-of-fit on F^2	1.139	0.836
final R indices [$I > 2\sigma(I)$]	$R1$ = 0.0386, $wR2$ = 0.0893	$R1$ = 0.0378, $wR2$ = 0.0813
R indices (all data)	$R1$ = 0.0448, $wR2$ = 0.0972	$R1$ = 0.0699, $wR2$ = 0.0855

diamagnetism using Pascal constants, and for the diamagnetic contribution of the sample holder by measurement.

DFT Calculations. Density functional calculations were carried out using the Gaussian 03 suite of programs,[41] with the Def2-SVP basis set on all atoms.[42] The crystallographically determined geometry was used in conjunction with the BP86[43] and B3LYP[44] exchange-correlation functionals to determine the ground state multiplicity of **2**.

■ ASSOCIATED CONTENT

Supporting Information. X-ray crystallography data in CIF format. B3LYP/Def2-SVP natural orbitals of compound **2**. This material is available free of charge via the Internet at http://pubs.acs.org.

■ AUTHOR INFORMATION

Corresponding Author

*E-mail: Richard.Layfield@manchester.ac.uk.

■ ACKNOWLEDGMENT

The authors acknowledge the support of the EPSRC, The EPSRC UK National Electron Paramagnetic Resonance Service at The University of Manchester, and The Royal Society. R.A.L. thanks the Alexander von Humboldt Foundation for the award of a Fellowship for Experienced Researchers.

■ REFERENCES

(1) (a) Andersen, R. A.; Faegri, K., Jr.; Green, J. C.; Haaland, A.; Lappert, M. F.; Leung, W.-P.; Rypda, K. *Inorg. Chem.* **1988**, *27*, 1782–1786. (b) Olmstead, M. M.; Power, P. P.; Shoner, S. C. *Inorg. Chem.* **1991**, *30*, 2547–2551.

(2) Lappert, M. F.; Protchenko, A.; Power, P. P.; Seeber, A. In *Metal Amide Chemistry*; John Wiley and Sons, Ltd.: Chichester, U.K., 2009; Chapter 6.

(3) Power, P. P. *Comments Inorg. Chem.* **1989**, *8*, 177–202.

(4) Bartlett, R. A.; Power, P. P. *J. Am. Chem. Soc.* **1987**, *109*, 7563–7564.

(5) Chen, H.; Bartlett, R. A.; Dias, H. V. R.; Olmstead, M. M.; Power, P. P. *J. Am. Chem. Soc.* **1989**, *111*, 4338–4345.

(6) Panda, A.; Stender, M.; Wright, R. J.; Olmstead, M. M.; Klavins, P.; Power, P. P. *Inorg. Chem.* **2002**, *41*, 3909–3916.

(7) Reiff, W. M.; Schulz, C. E.; Whangbo, M. H.; Seo, J. I.; Lee, Y. S.; Potratz, G. R.; Spicer, C. W.; Girolami, G. S. *J. Am. Chem. Soc.* **2009**, *131*, 404–405.

(8) Merrill, W. A.; Stich, T. A.; Brynda, M.; Yeagle, G. J.; Fettinger, J. C.; De Hont, R.; Reiff, W. M.; Schulz, C. E.; Britt, R. D.; Power, P. P. *J. Am. Chem. Soc.* **2009**, *131*, 12693–12702.

(9) Ellison, J. J.; Ruhlandt-Senge, K.; Power, P. P. *Angew. Chem., Int. Ed.* **1994**, *22*, 1178–1180.

(10) MacDonnell, F. M.; Ruhlandt-Senge, K.; Ellison, J. J.; Holm, R. H.; Power, P. P. *Inorg. Chem.* **1995**, *34*, 1815–1822.

(11) Bartlett, R. A.; Ellison, J. J.; Power, P. P.; Shoner, S. C. *Inorg. Chem.* **1991**, *30*, 2888–2894.

(12) Nehete, U. N.; Anantharaman, G.; Chandrasekhar, V.; Murugavel, R.; Walawalker, M. G.; Roesky, H. W.; Vidovic, D.; Magull, J.; Samwer, K.; Sass, B. *Angew. Chem., Int. Ed.* **2004**, *43*, 3832–3835.

(13) Chen, H.; Olmstead, M. M.; Pestana, D. C.; Power, P. P. *Inorg. Chem.* **1991**, *30*, 1783–1787.

(14) Verma, A. K.; Lee, S. C. *J. Am. Chem. Soc.* **1999**, *121*, 10838–10839.

(15) Duncan, J. S.; Nazif, T. M.; Verma, A. K.; Lee, S. C. *Inorg. Chem.* **2003**, *42*, 1211–1224.

(16) Sydora, O. L.; Wolczanski, P. T.; Lobkovski, E. B. *Angew. Chem., Int. Ed.* **2003**, *42*, 2685–2687.
(17) Ohki, Y.; Sunada, Y.; Honda, M.; Katsada, M.; Tatsumi, K. *J. Am. Chem. Soc.* **2003**, *125*, 4052–4053.
(18) Ohki, Y.; Sunada, Y.; Tatsumi, K. *Chem. Lett.* **2005**, *34*, 172–173.
(19) Sydora, O. L.; Henry, T. P.; Wolczanski, P. T.; Lobkovski, E. B.; Rumbovsky, E.; Hendrickson, D. N. *Inorg. Chem.* **2006**, *45*, 609–626.
(20) Ohki, Y.; Ikagawa, Y.; Tatsumi, K. *J. Am. Chem. Soc.* **2007**, *129*, 10457–10465.
(21) Pryadun, R.; Holm, R. H. *Inorg. Chem.* **2008**, *47*, 3366–3370.
(22) Ohki, Y.; Imada, M.; Murata, A.; Sunada, Y.; Ohta, S.; Honda, M.; Sasamori, T.; Tokitoh, N.; Katada, M.; Tatsumi, K. *J. Am. Chem. Soc.* **2009**, *131*, 13168–13178.
(23) Hauptmann, R.; Kliss, R.; Schneider, J.; Henkel, G. *Z. Anorg. Allg. Chem.* **1998**, *624*, 1927–1936.
(24) Hauptmann, R.; Kliss, R.; Henkel, G. *Angew. Chem., Int. Ed.* **1999**, *38*, 377–379.
(25) Dumestre, F.; Chaudret, B.; Amiens, C.; Renaud, P.; Fejes, P. *Science* **2004**, *303*, 821–823.
(26) Lacroix, L. −M.; Lachaize, S.; Falqui, A.; Respaud, M.; Chaudret, B. *J. Am. Chem. Soc.* **2009**, *131*, 549–557.
(27) (a) Layfield, R. A. *Chem. Soc. Rev.* **2008**, *37*, 1098–1107. (b) Alvarez, C. S.; Bond, A. D.; Harron, E. A.; Layfield, R. A.; Mosquera, M. E. G.; McPartlin, M.; Rawson, J. M.; Wright, D. S. *Dalton Trans.* **2003**, 3002–3008. (c) Alvarez, C. S.; Bond, A. D.; Cave, D.; Mosquera, M. E. G.; Harron, E. A.; Layfield, R. A.; McPartlin, M.; Rawson, J. M.; Wood, P. T.; Wright, D. S. *Chem. Commun.* **2002**, 2980–2981. (d) Aluarez, C. S.; Bond, A. D.; Harron, E. A.; Layfield, R. A.; McAllister, J. A.; Pask, C. P.; Rawson, J. M.; Wright, D. S. *Organometallics* **2001**, *20*, 4135–4138.
(28) Layfield, R. A.; McDouall, J. J. W.; Sulway, S. A.; Tuna, F.; Collison, D.; Winpenny, R. E. P. *Chem.—Eur. J.* **2010**, *16*, 4442–4446.
(29) Layfield, R. A.; Bashall, A.; McPartlin, M.; Rawson, J. M.; Wright, D. S. *Dalton Trans.* **2006**, 1660–1666.
(30) Bailey, P. J.; Pace, S. *Coord. Chem. Rev.* **2001**, *214*, 91–141.
(31) (a) Foley, S. R.; Yap, G. P. A.; Richeson, D. S. *Chem. Commun.* **2000**, 1515–1516. (b) Foley, S. R.; Yap, G. P. A.; Richeson, D. S. *Inorg. Chem.* **2002**, *41*, 4149–4157. (c) Rose, R. P.; Jones, C.; Schulten, C.; Aldridge, S.; Stasch, A. *Chem.—Eur. J.* **2008**, *14*, 8477–8480.
(32) Oakley, S. H.; Coles, M. P.; Hitchcock, P. B. *Inorg. Chem.* **2004**, *43*, 7564–7566.
(33) (a) Cotton, F. A.; Gruhn, N. E.; Gu, J.; Huang, P.; Lichtenberger, D. L.; Murillo, C. A.; Van Dorn, L. O.; Wilkinson, C. C. *Science* **2002**, *298*, 1971–1974. (b) Cotton, F. A.; Gruhn, N. E.; Lichtenberger, D. L.; Murillo, C. A.; Timmons, D. J.; Van Dorn, L. O.; Villagrán, D.; Wang, X. *Inorg. Chem.* **2006**, *45*, 201–213. (c) Cotton, F. A.; Daniels, L. M.; Murillo, C. A.; Timmons, D. J.; Wilkinson, C. C. *J. Am. Chem. Soc.* **2002**, *124*, 9249–9256. (d) Cotton, F. A.; Murillo, C. A.; Reibenspies, J. H.; Villagrán, D.; Wang, X.; Wilkinson, C. C. *Inorg. Chem.* **2004**, *43*, 8373–8378. (e) Fernandez-Cortabitarte, García, F.; Morey, J. V.; McPartlin, M.; Singh, S.; Wheatley, A. E. H.; Wright, D. S. *Angew. Chem., Int. Ed.* **2007**, *46*, 5425. (f) Chisholm, M. H.; Gallucci, J.; Hadad, C. M.; Huffma, J. C.; Wilson, P. J. *J. Am. Chem. Soc.* **2003**, *125*, 16040–16049. (g) Cotton, F. A.; Dalal, N. S.; Huang, P.; Ibragimov, S. A.; Murillo, C. A.; Piccoli, P. M. B.; Ramsey, C. M.; Schultz, A. J.; Wang, X.; Zhao, Q. *Inorg. Chem.* **2007**, *46*, 1718–1726. (h) Berry, J. F.; Cotton, F. A.; Huang, P.; Murillo, C. A.; Wang, X. *Dalton Trans.* **2005**, 3713–3715. (i) Irwin, M. D.; Abdou, H. E.; Mohamed, A. A.; Fackler, J. P., Jr. *Chem. Commun.* **2003**, 2882. (j) Cotton, F. A.; Murillo, C. A.; Wang, X.; Wilkinson, C. C. *Dalton Trans.* **2007**, 3943–3951.
(34) Allan, F. H. *Acta Crystallogr., Sect. B: Struct. Sci.* **2002**, *B58*, 380–388.
(35) Collison, D.; McInnes, E. J. L.; Brechin, E. K. *Eur. J. Inorg. Chem.* **2006**, 2725–2733.
(36) (a) Wunderlich, S. H.; Knochel, P. *Angew. Chem., Int. Ed.* **2009**, *48*, 9717–9720. (b) Alborés, P.; Carrella, L. M.; Clegg, W.; García-Á lvarez, P.; Kennedy, A. R.; Klett, J.; Mulvey, R. E.; Rentschler, E.; Russo, L. *Angew. Chem., Int. Ed.* **2009**, *48*, 3317–3321.
(37) (a) Lambert, C.; Hampel, F.; von R. Schleyer, P. *J. Organomet. Chem.* **1993**, *455*, 29–35. See also: (b) Andrews, P. C.; Clegg, W.; Mulvey, R. E.; O'Neill, P. A.; Wilson, H. M. M. *J. Chem. Soc., Chem. Commun.* **1993**, 1142−1143.
(38) (a) Mulvey, R. E. *Chem. Soc. Rev.* **1998**, *27*, 339–346. (b) Mulvey, R. E. *Chem. Soc. Rev.* **1991**, *20*, 167–209. (c) Armstrong, D. R.; Barr, D.; Clegg, W.; Hodgson, S. M.; Mulvey, R. E.; Reed, D.; Snaith, R.; Wright, D. S. *J. Am. Chem. Soc.* **1989**, *111*, 4719–4727.
(39) Borrás-Almenar, J. J.; Clemente-Juan, J. M.; Coronado, E.; Tsukerblat, B. S. *J. Comput. Chem.* **2001**, *22*, 985–991.
(40) Andres, H.; Bominaar, E. L.; Smith, J. M.; Eckert, N. A.; Holland, P. L.; Münck, E. *J. Am. Chem. Soc.* **2002**, *124*, 3012–3025.
(41) Frisch, M. J.; et al. Gaussian 03, Revision E.01; Gaussian, Inc.: Wallingford, CT, 2004.
(42) Weigend, F.; Ahlrichs, R. *Phys. Chem. Chem. Phys.* **2005**, *7*, 3297.
(43) (a) Becke, A. D. *Phys. Rev. A* **1988**, *38*, 3098. (b) Perdew, J. P. *Phys. Rev. B* **1986**, *33*, 8822. (b) Becke, A. D. *J. Chem. Phys.* **1993**, *98*, 5648.
(44) (a) Mayer, I. *Chem. Phys. Lett.* **1983**, *97*, 270. (b) Mayer, I. *Int. J. Quantum Chem.* **1984**, *26*, 151.